Chalcogenide Letters Vol. 18, No. 8, August 2021, p. 449 - 455

A method for preparing high-quality PbS thin films

W. L. Jiang, H. Deng*, Q. Feng, X. Y. Li
University of Electronic Science and Technology of China, Chengdu 610054, China

High-quality lead sulfide (PbS) thin films were successfully synthesized by chemical bath deposition (CBD) method. X-ray diffraction (XRD) and scanning electron microscope (SEM) results indicated that the films had face-centered cubic (FCC) structures with strong (200) preferred orientation and high-quality crystals. The band gap of the films was about 0.65eV, which had an obvious broadening. Then I-V characteristic curve and relative response were measured, respectively. It was found that the films had good photosensitivity. Since the films had high crystallinity and preferred orientation, it was expected to achieve better practical effects in the field of infrared applications.

(Received April 28, 2021; Accepted August 7, 2021)

Keywords: PbS thin films, CBD, Optical properties, Photosensitivity, Relative response

1. Introduction

Due to the unique optoelectronic properties of semiconductor materials, binary and ternary semiconductor compounds have been studied deeply in recent years [1]. As an important narrow band gap semiconductor compound, PbS has been extensively used in gas sensors [2], solar cells [3-5], infrared detectors [6,7] and other fields due to its advantages of relatively narrow energy band gap (about 0.41eV at 300K) [8], up to 18nm exciton Bohr radius [9], and excellent photoconductive properties in the near-infrared band at room temperature [10].

Currently, the main application forms of PbS in devices are thin films structures, in which the surface microstructures of the films directly affect the performance of the device, while the preparation process of the films is closely related to the surface microstructures. Therefore, how to successfully prepare high-quality PbS thin films has become the focus of more and more researchers. Different synthesis processes have been developed to synthesize PbS thin films with uniform particles and good morphology, including electrochemical [11], spray pyrolysis [12-14], electrodeposition [15], chemical bath deposition (CBD) [16], vacuum evaporation [17], microwave assisted heating [18], successive ionic layer adsorption and reaction (SILAR) [19-21]. The films prepared by physical methods are of high qualities, but the high production cost and huge energy consumption limit their further developments; the chemical methods are relatively more efficient and environmental protection. CBD technology as an important chemical method is widely used because of its simple process and strong controllability. Meanwhile, the morphology of PbS particles can be well controlled by adjusting the PH, concentration and selecting the appropriate complexing agent [22-24].

* Corresponding author: hdeng@uestc.edu.cn
https://doi.org/10.15251/CL.2021.188.449

In this article, high-quality PbS thin films were successfully synthesized by strictly controlling the reaction conditions. Then the surface morphology and microstructure of the sample were analyzed by using related characterization tools. The I-V characteristic curve and relative response of the films were investigated at last, and the experimental results were further explained.

2. Experimental

In this experiment, the reagents used were of analytical grade unless otherwise specified. In a typical synthesis process, the concentration ratio of lead nitrate ($Pb(NO_3)_2$), sodium hydroxide (NaOH) and thiourea ($SC(NH_2)_2$) was fixed at 1:3:1. First, add appropriate amounts of deionized water to the weighed three reactants respectively, and stir to dissolve them. Then the NaOH solution was slowly poured into $Pb(NO_3)_2$ solution, stirred gently to make the reaction fully proceed, and the supernatant was taken out after standing. The cleaned glass slides were vertically placed into $SC(NH_2)_2$ solution with a constant temperature of 30℃. The supernatant obtained before was poured into $SC(NH_2)_2$ solution and deposited for 60min. After deposition, the gold electrodes were evaporated and the size of the photosensitive surface was 3mm×3mm.

The structural characterization was performed by Bede D1 diffractometer with Cu-Kα (λ = 1.54056Å) radiation for the 2Θ changing from 20° to 60°. Surface morphologies of the obtained films were investigated using JSM-6490lv scanning electron microscopy, which operates at 20KV. The Raman spectrum was recorded using a spectrometer (Horiba iHR 550) with a 532nm laser incident. The transmission spectrum was determined by Lambda 750 spectrophotometer. HZ-220 V-250 W infrared lamp was used as the radiation source. X-Y recorder was used to determine the I-V characteristic curve of the films. The relative response was measured by the spectral response testing system (Vendor: Zolix, China).

3. Results and discussion

X-ray diffraction spectrum of the obtained films had shown as Fig. 1(a). Compared with the standard card library of cubic structure PbS, it was consistent with the standard card (JCPDS No. 5-592), and the corresponding growth crystal planes were (111), (200), (311), respectively, while other diffraction peaks such as (220), (222) were not detected due to the weak intensity. It was not difficult to find from the figure that the films had FCC structures with (200) preferred orientation. The main diffraction peak was located at 2θ=30.15°, and the corresponding intensity and half-height width (FWHM) were 780 and 0.1988°, respectively. Since the films had better preferred orientation, the grain size could be determined by the Debye-Scherrer formula given below [25]:

$$D = k\lambda/\beta cos\theta \quad (1)$$

where k=0.89; λ=0.154056nm; θ and β were the diffraction angle and FWHM, respectively. Substituting the relevant parameters into the equation (1), the grain size of the films was calculated to be 40.92nm.

The surface morphology of the sample was characterized, and the result was shown in Fig. 1(b). It was found that the films obtained had a typical morphology of cubic crystal phase PbS, the square particles were uniformly stacked on the glass substrate, and there was no clear crack between the particles, indicating that the prepared films had high qualities. The results of structure and morphology analysis together showed that the films prepared owned (200) preferred orientation and high-quality crystallization.

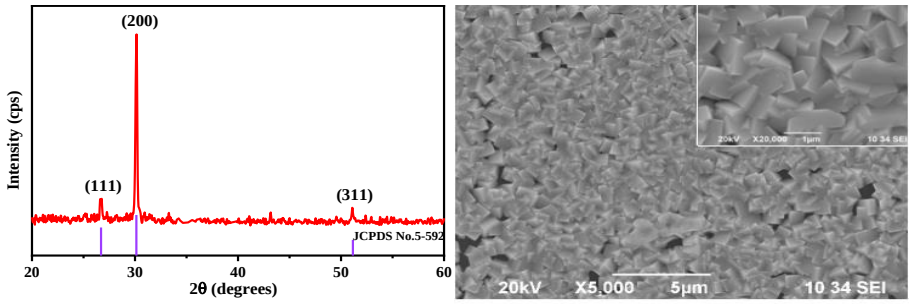

Fig. 1. (a) and (b) are the XRD patterns and SEM morphologies of the films, respectively

Raman spectroscopy is a test method to quickly identify the characteristics of crystal materials, which can effectively reflect the vibration mode of materials. According to the Fig.2, there were four peaks in the measured wavenumber range, located at 429, 602, 970 and 1041cm^{-1}, respectively. The vibration peaks at 429 and 602cm^{-1} were characteristic peaks of PbS, corresponding to the 2LO and 3LO phonon modes, respectively. [26, 27] The vibration peaks at 970 and 1041cm^{-1} could be attributed to the oxidation of the sample due to the high heat of the laser, resulting in the formation of PbO and $PbSO_4$.[28] Since all the peaks appearing corresponded to the typical vibration mode of PbS, it indicated that the obtained films had higher purity. In addition, the narrower width and higher intensity of the vibration peak indicated that the sample had better crystalline quality. The Raman spectrum further proved the test results of XRD and SEM, reflecting the higher quality of the obtained films.

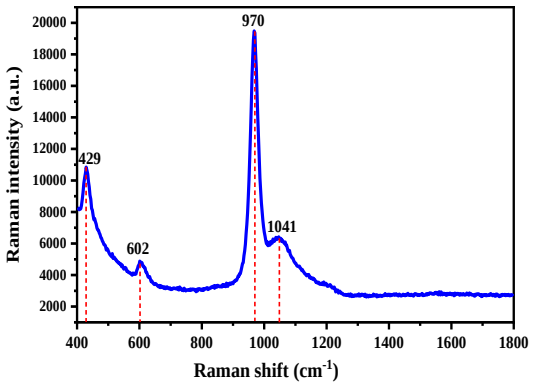

Fig. 2. The Raman characterization spectrum of the films

In Fig. 3(a), we plotted the transmission spectrum of PbS thin films. According to the change trend, the test range could be divided into three areas. The transmittance showed a downward trend in the range of 1900-2500nm and 800-1500nm; while in the wavelength range of 1500-1900nm, the transmittance almost remained unchanged. Since the transmittance was inversely proportional to the absorptance, its main absorption peak was approximately located at 1900nm. The change curve of $(\alpha hv)^2$ with hv shown in Fig. 3(b) was determined by the Tauc formula given below [29]:

$$(\alpha hv)^{1/n} = A(hv - E_g) \tag{2}$$

where α is the light absorption coefficient; hv is the incident photon energy; E_g is the band gap of the material; since PbS is a narrow band gap semiconductor material with direct transition, n=1/2. The intercept that extends the linear part of the curve to the horizontal axis is the band gap of the material, which was 0.64516eV. Compared with bulk material, the band gap is 0.41eV, and the absorption peak is located at 3024nm [30, 31]. The band gap of the obtained PbS films was obviously broadened, and the absorption peak moved to the short-wave direction. It was speculated that the reason for this phenomenon might be due to the reduction of particle size, which changed the optical properties of the material.

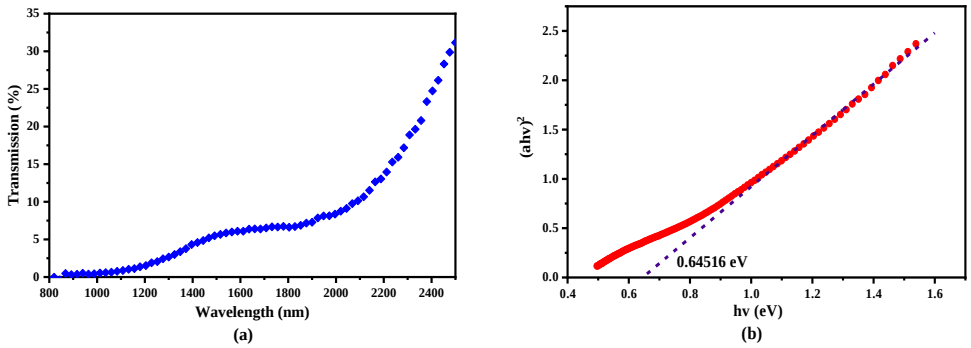

Fig. 3. (a) showed the optical transmission spectrum of PbS thin films. (b) The change curve of $(\alpha hv)^2$ *versus* hv

The I-V characteristic curve and relative response of the films were measured with the structure shown in Fig. 4(a), in which the films were used to convert the incident light signals into electrical signals. Fig. 4(b) showed the I-V characteristic curves of the films under dark and light conditions. It was found that the current and voltage had a linear relationship regardless of external radiation, indicating that PbS thin films could be regarded as a photoresistor and formed an ohmic contact with the gold electrodes. According to the figure, it could be calculated that under a bias voltage of 2000mV, the light and dark currents of the films were 0.2427mA and 0.1604mA, respectively, and the current change rate of the films under this test condition was 51.31%. It can be seen from the above results that due to the good preferred orientation and high crystallinity of the obtained films, it has better photosensitivity and can respond effectively to changes in external incident illumination.

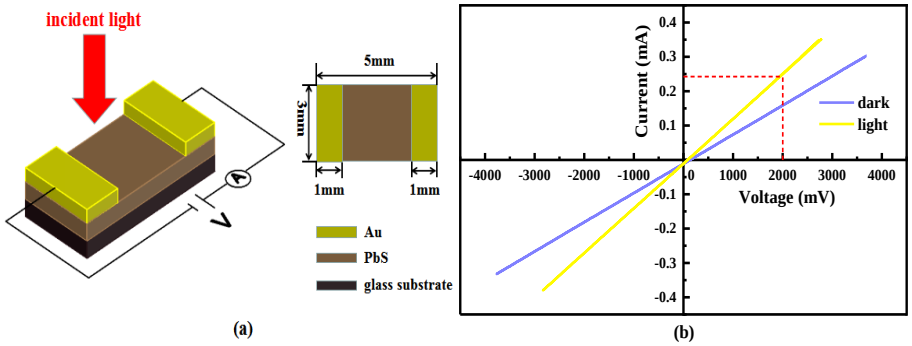

Fig. 4. (a) Structure diagram of PbS thin film performance test. (b) I-V characteristic curves of PbS thin films under dark and exposure conditions

Since the structure directly affects the performance of the films, the quality of the sample can also be reflected laterally by measuring its relative response. The photocurrent and relative response were measured respectively by spectral response measurement system.

The experimental results showed that the peak value of photocurrent appeared around 1300nm, but the photocurrent in the near-infrared band showed a downward trend instead (Fig. 5(a)), which was undesirable. It is speculated that the power of brominated tungsten lamp in this band range is reduced, which leads to the decrease of external irradiance. Meanwhile, the imported Si detector (manufactured by UDT Sensor, USA) was used as the standard detector to calibrate the light source, and the relative response of the films was measured, as shown in Fig. 5(b). It was found that the sample can respond effectively within the test range, and its peak wavelength was at 2200nm, which reflects the high quality of the prepared films. The measurement results indicate that the obtained films have high responsiveness to the near-infrared band, which is expected to achieve better practical effects in the field of infrared applications.

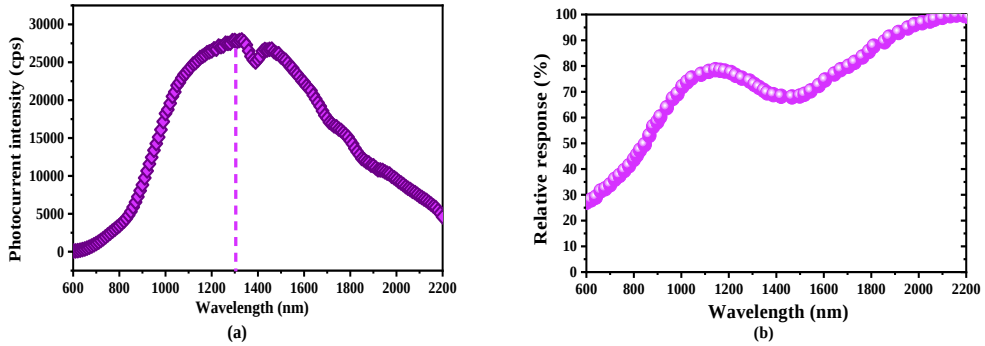

Fig. 5. (a) and (b) are the photocurrent and relative response curves of the films, respectively

4. Conclusion

High-quality PbS thin films were successfully synthesized by strictly controlling the reaction conditions. Structure and morphology analysis showed that the films had FCC structures with (200) preferred orientation and high-quality crystallization. Photosensitivity study revealed

that the films could respond effectively to changes in the external incident illumination, with a sensitivity of 51.31%. Compared with the bulk band gap of 0.41eV, the band gap of the obtained films was 0.65eV, which had a significant broadening. Since the films had high crystallinity and preferred orientation, it was expected to achieve better practical effects in the field of infrared applications.

Acknowledgements

This work was supported by the National High-tech Programs [grant number G060103019].

References

[1] D. K. Sonavane, S. K. Jare, R. V. Kathare, R. N. Bulakhe, J. J. Shim, Materials Today: Proceedings **5**(2), 7743 (2018).
[2] S. T. Navale, D. K. Bandgar, M. A. Chougule, V. B. Patil, RSC. Adv **5**(9), 6518 (2015).
[3] S. R. Rosario, I. Kulandaisamy, K. D. A. Kumar, K. Ramesh, H. A. Ibrahium, N. S. Awwad, Int. J. Energy. Res. **44**(6), 4505 (2020).
[4] Y. B. Castillo-Sánchez, L. A. González, Mater. Sci. Semicond. Process **121**, 105405 (2021).
[5] A. Ekinci, Ö. Şahin, S. Horoz, J. Mater. Sci.-Mater. Electron. **31**, 1210 (2020).
[6] E. K. Ampadu, J. D. Kim, E. S. Oh, D. Y. Lee, K. S. Kim, Mater. Lett. **277**, 128323 (2020).
[7] D. I. Halge, V. N. Narwade, P. M. Khanzode, J. W. Dadge, A. S. Rana, K. A. Bogle, AIP Conference Proceedings **2220**, 020021 (2020).
[8] E. Yücel, Y. Yücel, Ceram. Int. **43**(1), 407 (2017).
[9] T. Tohidi, K. Jamshidi-Ghaleh, A. Namdar, R. Abdi-Ghaleh, Mater. Sci. Semicond. Process. **25**, 197 (2014).
[10] E. Pentia, L. Pintilie, I. Matei, T. Botila, I. Pintilie, Infrared Phys. Technol. **44**(3), 207 (2003).
[11] M. Alanyalıoğlu, F. Bayrakceken, Ü. Demir, Electrochim. Acta **54**(26), 6554 (2009).
[12] S. Ravishankar, A. R. Balu, K. Usharani, S. Balamurugan, D. Prabha, V. S. Nagarethinam, Optik **134**, 121 (2017).
[13] S. RaviShankar, A.R. Balu, M. Anbarasi, V. S. Nagarethinam, Optik **126**(20), 2550 (2015).
[14] C. Rajashree, A. R. Balu, Optik **127**(20), 8892 (2016).
[15] W. Han, L. Y. Cao, J. F. Huang, J. P. Wu, Mater. Technol. **24**(4), 217 (2009).
[16] S. Jana, R. Thapa, R. Maity, K. K. Chattopadhyay, Physica E: Low-dimensional Systems and Nanostructures **40**(10), 3121 (2008).
[17] S. Kumar, T. P. Sharma, M. Zulfequar, M. Husain, Physica B: Condensed Matter **325**, 8 (2003).
[18] A. S. Obaid, M. A. Mahdi, Y. Yusof, M. Bououdina, Z. Hassan, Mater. Sci. Semicond. Process **16**(3), 971 (2013).
[19] E. Yücel, Y. Yücel, B. Beleli, J. Cryst. Growth. **422**, 1 (2015).
[20] J. Puišo, S. Lindroos, S. Tamulevičius, M. Leskelä, V.Snitka, Thin Solid Films **428**(1-2), 223 (2003).

[21] J. Puišo, S. Lindroos, S. Tamulevičius, M. Leskelä, V. Snitka, Solid State Phenomena **94**, 261 (2003).
[22] A. N. Chattarki, S. S. Kamble, L. P. Deshmukh, Mater. Lett. **67**(1), 39 (2012).
[23] A. K. Yildirim, B. Altiokka, Emerg. Mater. Res. **9**(1), 47 (2020).
[24] B. Abdallah, R. Hussein, N. Al-Kafri, W. Zetoun, Iranian Journal of Science and Technology Transactions A: Science **43**, 1371 (2019).
[25] E. Yücel, N. Güler, Y. Yücel, J. Alloy. Compd. **589**, 207 (2014).
[26] V. Singh, D. Joung, L. Zhai, S. Das, S. I. Khondaker, S. Seal, Prog. Mater. Sci. **56**(8), 1178 (2011).
[27] Y. H. Zhang, L. Guo, P. G. Yin, R. Zhang, Q. Zhang, S. H. Yang, Chem.-Eur. J. **13**(10), 2903 (2007).
[28] Y. Batonneau, C. Bremard, J. Laureyns, J. C. Merlin, J. Raman Spectrosc. **31**(12), 1113 (2000).
[29] L. Beddek, M. Messaoudi, N. Attaf, M.S. Aida, J. Bougdira, J. Alloy. Compd. **666**, 327 (2016).
[30] E. V. Nikolaeva, S. A. Ozerin, A.E. Grigoriev, E. I. Grigoriev, S. N. Chvalun, G. N. Gerasimov, L. I. Trakhtenberg, Materials Science and Engineering: C. **8–9**(1), 217 (1999).
[31] B. Altiokka, Arab J. Sci. Eng. **40**, 2085 (2015).